IEEE Access
Multidisciplinary ⋮ Rapid Review ⋮ Open Access Journal

Received June 16, 2021, accepted June 28, 2021, date of publication June 30, 2021, date of current version July 8, 2021.

Digital Object Identifier 10.1109/ACCESS.2021.3093775

A Review of Reconfigurable Leaky-Wave Antennas

NIMA JAVANBAKHT[1], (Member, IEEE), BARRY SYRETT[1], (Member, IEEE), RONY E. AMAYA[1], (Senior Member, IEEE), AND JAFAR SHAKER[2], (Senior Member, IEEE)

[1]Department of Electronics, Carleton University, Ottawa, ON K1S 5B6, Canada
[2]Communication Research Center, Ottawa, ON K2K 2Y7, Canada

Corresponding author: Nima Javanbakht (nima.javanbakht@carleton.ca)

This work was supported in part by the Natural Science and Engineering Research Council of Canada (NSERC).

ABSTRACT A comprehensive survey of the reconfigurable leaky-wave antennas (LWAs) is made in this paper. Beam-steering and unique radiating features of LWA are highlighted particularly. Therefore, the radiation mechanism of different types of LWA, including uniform, quasi-uniform, periodic, and metamaterial LWAs are discussed in detail. The guiding structures for realizing LWAs, namely microstrip, waveguide, substrate integrated waveguide (SIW), and half-mode SIW (HMSIW) are investigated as well. Basic concepts of electronic beam-scanning LWAs are also introduced, and several state-of-the-art reconfigurable LWAs are studied thoroughly. The investigated reconfigurable LWAs are suitable for beam-scanning applications due to their compactness, ease of implementation, reasonably high gain, and relatively wide beam-scanning range, as will be demonstrated through this comprehensive review.

INDEX TERMS Antenna, compact, leaky-wave, microstrip, reconfigurable, waveguide.

I. INTRODUCTION

Leaky-wave antennas (LWAs) are among the beam-scanning antennas. A large body of research has been carried out on LWAs since the 1950s [1]. The radiation of these antennas occurs through the leakage of a travelling wave propagating through a guiding structure [1]–[5]. Hence they are labelled ‘‘leaky-wave antenna.’’

Microstrip and waveguide are the primary choices as the guiding structures for realizing the LWAs. Microstrip-based LWA suffers from high dielectric loss [1]–[5]. On the other hand, waveguide-based LWA is bulky and unsuitable for miniaturized applications [1]–[5]. Substrate integrated waveguide (SIW) was introduced as a suitable candidate for the realization of miniaturized applications [5]–[9]. SIW is a low-profile rectangular waveguide in which the sidewalls are replaced by via fences to confine the fields [5]–[7]. The advantages of SIW technology, such as ease of fabrication and compact size [5]—[9], lead to broad applications in microwave circuits and antennas. Removing half of the top conductor cladding leads to a more compact structure called half-mode substrate integrated waveguide (HMSIW) [10]–[19]. In the HMSIW LWA, the leaky-wave leaks into space through the aperture [10]–[15] and the slots on the surface [16], [17]. HMSIW- and SIW-based antennas can be fabricated using a printed circuit board (PCB), low temperature co-fired ceramic (LTCC), or electronic printing technology. LWA can also be integrated into silicon-based structures [20] to achieve a miniaturized transceiver. LWA can be realized on the dielectric waveguide [21] dielectric image line [22], wedge-like waveguide [23], gap waveguides [24]–[27], and corrugated SIW [28] for mm-wave and X-band applications. A dielectric waveguide is a dielectric-based guiding structure without conducting walls. A gap waveguide is a metallic waveguide consisting of several variable conducting pins, which are machined using the CNC machine. Compactness and simple reconfigurability mechanism, by controlling the height and spacing between pins, put the gap waveguide at an advantage compared to the conventional waveguide for realizing LWA [27]. Corrugated SIW is a SIW in which open circuit stubs replace the via fences, reducing the cost and difficulty of the fabrication [28].

The associate editor coordinating the review of this manuscript and approving it for publication was Raghvendra Kumar Chaudhary.

While LWA is mainly used as a beam-scanning antenna, it can also be implemented as a band-pass microwave filter [29] and multiplexer [30]. Most of the reported LWAs in the literature are unidirectional antennas, but bidirectional LWA can be designed by implementing different excitation ports [31]. It should be noted that LWA is also a suitable candidate as the on-chip antenna in CMOS and Silicon-based technology at sub-THz frequency bands, noting the relaxed metal density rules [20].

The structure of this paper is as follows. First, the radiation mechanism of LWA, guiding structures, and different types of LWAs are introduced in section II. Then, several reconfigurable LWAs are investigated thoroughly in section III, and a comparison between state-of-the-art reconfigurable LWAs is made in section IV.

II. LEAKY-WAVE ANTENNA

Realizing beam-steerable and high gain antennas is crucial for overcoming path loss and vulnerability to environmental variations [32]. LWA is a traveling wave antenna [1]–[5]. These antennas are called leaky-wave since the propagating wave gradually leaks into space through the discontinuities [1]–[5], as demonstrated in Fig. 1. The discontinuities (*i.e.,* radiator) are often slots on the surface of a conductive waveguide or strip lines over a dielectric substrate [1]–[3]. As stated before, the guiding structure can be a dielectric substrate or a metallic waveguide.

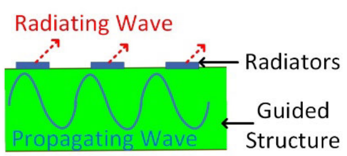

FIGURE 1. Leakage mechanism of an LWA.

Beam-steering capability, wide impedance bandwidth, high gain, low cost, ease of fabrication, and compactness are among the advantages of LWAs compared to other high gain beam-steerable antennas such as phased array antennas [4], [6], [33], [34]. The beam-scanning in the LWA can be achieved through frequency, mechanical, or electronic beam-scanning, as presented in Fig. 2. LWA and phased array antenna [1]–[3] are two alternatives for beam-steering, and the preference of one technology over the other depends on the targeted application. LWA achieves beam-scanning without the requirement of having a complex feed network and phase shifters. Hence, LWA is cheaper and easier to fabricate than the phased array. However, controlling LWA's attenuation and phase constants individually is very difficult. In other words, there are more degrees of freedom for controlling the radiation pattern of the phased array antenna.

Dispersion analysis is the first crucial step in the design of LWA. Dispersion characteristic is defined as the complex propagation constant throughout the frequency band [35], [36]. A dispersion diagram of a typical

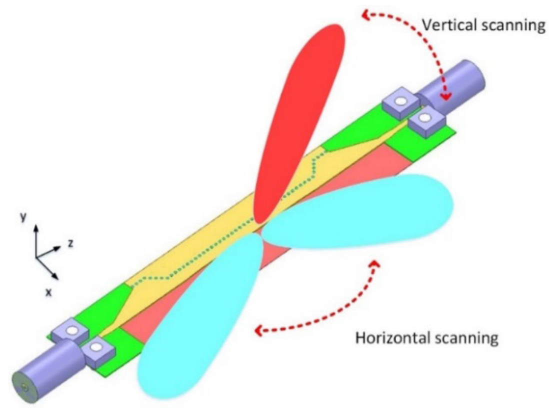

FIGURE 2. Beam-scanning in an LWA.

waveguide-based antenna exhibiting several Floquet modes (*i.e.,* space harmonics) is presented in Fig. 3. As observed in Fig. 3, higher-order Floquet modes are the shifted version of the fundamental ($n = 0$) mode [35]. In a waveguide-based periodic structure, the phase constants of fundamental (β_0) and higher order (nth) Floquet modes (β_n) are calculated by

$$\beta_n = \beta_0 + \frac{2\pi n}{p} \tag{1}$$

$$\beta_0 \cong k_0\sqrt{\varepsilon_r}\sqrt{1-\left(\frac{f_c}{f}\right)^2} \tag{2}$$

where β_0, n, p, ε_r, k_0, and f_c are phase constant of the fundamental Floquet mode, the number of the Floquet mode, period, relative permittivity, the free-space wavenumber, and cutoff frequency, respectively [35]. Similar to the waveguide modes, Floquet modes have cutoff frequencies determined by the spacing between elements (*i.e.,* period). Often it is desired to have only one mode propagates. This can be accomplished by tuning the dielectric constant, period, and frequency range [35], [36]. An LWA radiates if it operates in the fast-wave region [1], [2], where $-k_0 < \beta < k_0$. In the fast-wave region, the phase velocity is greater than the velocity of light in free space. This the reason that the propagating wave in this region is called fast-wave. In the slow-wave region, the propagating wave is evanescent, attenuating quickly. The airlines with negative and positive slopes (*i.e.,* $\beta = \pm k_0$) represent backward and forward endfires, respectively. While the frequency axis represents the broadside (*i.e.,* $\beta = 0$). The main-lobe pointing angle (θ_0) is calculated from

$$\cos(\theta_0) = \frac{\beta_n}{k_0} \tag{3}$$

It should be noted that θ_0 is measured from the forward endfire (*i.e.,* $\theta_0 = 0°$ is at the forward endfire). The length of the radiating section was extracted from

$$\Delta\theta = \frac{\lambda_0}{L_r \sin\theta_0} \tag{4}$$

where $\Delta\theta$, L_r, and λ_0 are half-power beamwidth (HPBW), radiation length, and free space wavelength, respectively

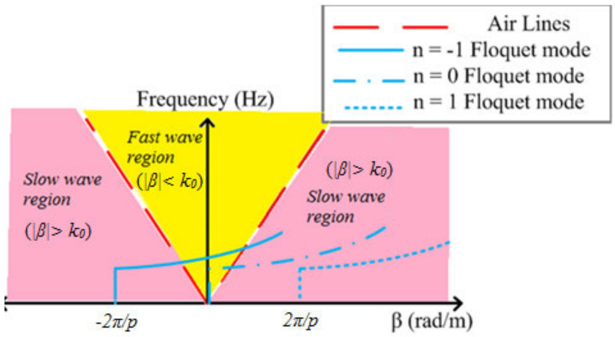

FIGURE 3. Dispersion diagram of a typical waveguide LWA.

[1], [2]. According to (3), beam-scanning occurs by changing the phase constant β_n, which lays the foundation of the beam-scanning mechanism in an LWA. According to (3) and (4), the HPBW reduces by approaching the broadside region. On the other hand, approaching the endfire results in a larger HPBW [1], [2]. LWA scans backward by exciting negative higher-order Floquet modes [1], [2], [37]. It should be noted that higher-order modes can be used to achieve full-space beam-scanning [38], enhance the antenna gain [8], and improve the radiation efficiency at the sub-THz frequency band [39].

As stated before, waveguide and microstrip structures are widely used as the guiding structures for realizing LWAs [1]–[5], [40]. A microstrip structure has an inherently considerable dielectric loss. On the other hand, waveguides are bulky and not suitable for integration and miniaturization purposes. SIW [6], [41]–[44] is widely used in mm-wave applications due to its remarkable benefits, such as ease of fabrication, integration capability, compactness, and low cost. Hence, SIW is a suitable candidate as the guiding structure of the LWA [45]–[61]. Via holes in a SIW can be utilized to emulate the operation of a dielectric-filled rectangular waveguide [6], [41]–[44], [62]–[64], as illustrated in Fig. 4. The via fences are in the shape of cylindrical holes filled with a conductive resin such as silver paste. The via fences act as the waveguide's sidewalls that confine the electric field of the TE_{n0} mode. In other words, SIW can only confine TE_{n0} modes since the surface current of these modes is not disturbed by the vias [6], [41], [42].

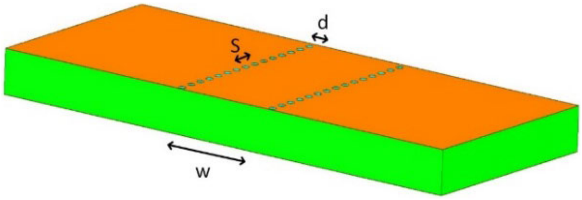

FIGURE 4. Conventional SIW.

Confinement of the electric field of the TE_{n0} modes in a SIW can be achieved by adjusting the diameters of the vias (d) to be larger than one-third of the via spacing (s) and smaller than one-fifth of the width (transverse spacing of the via fences) (w) [6], [41]. The effective width of the structure (w_{eff}) and the cutoff frequency (f_c) of the dominant mode (TE_{10}) are calculated by

$$w_{eff} = w - 1.08\frac{d^2}{s} + 0.1\frac{d^2}{w} \tag{5}$$

$$f_c = \frac{c}{2w_{eff}\sqrt{\varepsilon_r}} \tag{6}$$

where w_{eff}, w, d, s, c, and ε_r are the effective width, width, via diameter, via spacing, the velocity of light, and permittivity, respectively [6], [65], [66]. SIW has the same guided wave properties as a dielectric-filled rectangular waveguide [6]. SIW is inherently a periodic structure that can suffer from the band-stop issue. Furthermore, if the via spacing is not set correctly, leakage can occur from the via fence due to the periodic gaps [6]. SIW can be fed using surface-mounted or through-hole connectors. However, through-hole connectors are not suitable for a low-profile structure. Implementing a surface-mounted connector requires a microstrip transition to transfer signal from coaxial connector to SIW. Unfortunately, the microstrip transition has undesired effects on the radiation pattern at high frequency bands such as the mm-wave band [67].

LWAs are divided into three categories: uniform LWA (ULWA), quasi-uniform LWA (QLWA), and periodic LWA (PLWA) [1]–[5]. A ULWA has a uniform cross-section along the structure. A slot-based ULWA usually contains a single longitudinal long slot, as presented in Fig. 5(a). A ULWA can only scan the forward quadrant, *i.e.,* from broadside to forward endfire [1]–[5], [45]–[47], [48]. This is because only the fundamental Floquet mode ($n = 0$) propagates in the ULWA. The SLL of a ULWA can be reduced by tapering the via fence and the slot, as shown in Fig. 6 [45], [47]. The SLL was reduced to −40 dB [45] and −23.2 dB [47] by tapering the via fence and shape of the slot.

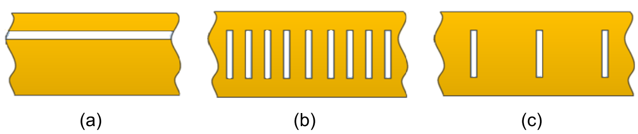

FIGURE 5. Schematic view of different types of an LWA. (a) ULWA, (b) QLWA, and (c) PLWA.

A QLWA contains several closely-spaced radiating elements, as illustrated in Fig. 5(b). Since the period is small, the cross-section can be considered uniform [1]–[5]. The small period of the slots assures that only the fundamental Floquet mode propagates. Hence, this antenna only scans the forward quadrant [1]–[5], [9], [49]–[51]. A SIW-based QLWA with transversal slots was introduced in [49] for the first time, as shown in Fig. 7. In [49], tapered slots and via fences at both ends of the antenna were implemented to improve the return loss. The SLL of a QLWA can be reduced by tapering the via fence and length of the transverse slots, as demonstrated in Figs. 8 and 9 [50], [9]. Tapering the slots in a shape of a fish led to an SLL reduction of about

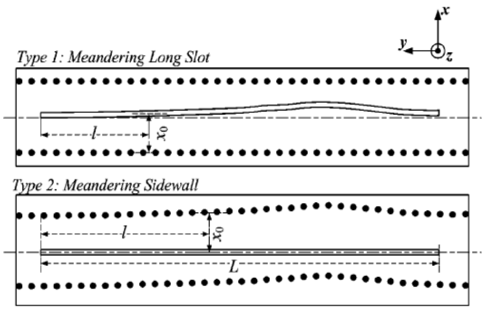

FIGURE 6. Proposed ULWA with reduced SLL in [45] ©2011 IEEE.

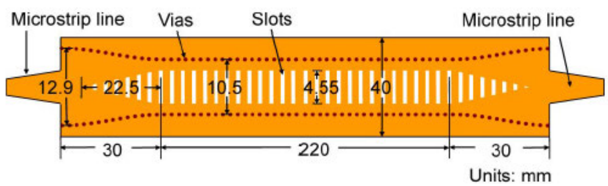

FIGURE 7. The first reported SIW QLWA [49] ©2012 IEEE.

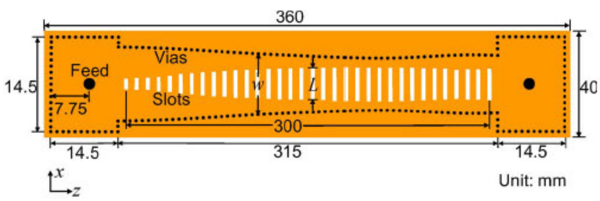

FIGURE 8. Tapered SIW QLWA with reduced SLL [50] ©2014 IEEE.

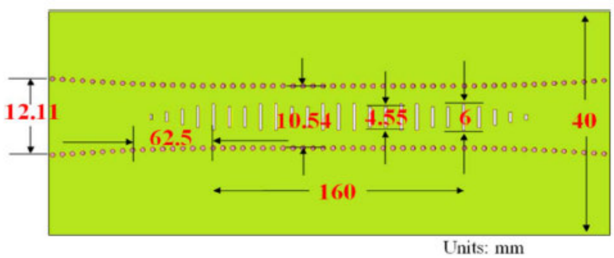

FIGURE 9. Butterfly-shaped QLWA with reduced SLL [9] ©2014 IEEE.

20 dB [50]. While tapering them in an eight-wing butterfly shape resulted in an SLL of about −14 dB [9]. Changing the spacing of transverse slots leads to SLL reduction of about 20 dB [51], as presented in Fig. 10. Furthermore, it is possible to design SIW LWA in conformal configuration, as illustrated in Fig. 11, for mounting on the plane fuselage and vehicle body [52]. Most of the reported LWAs in literature are a single antenna, whereas placing LWAs in the array configuration can be beneficial. For example, placing SIW QLWA in a hexangular array configuration, as shown in Fig. 12, leads to an omnidirectional coverage in the azimuth and frequency beam-scanning in the elevation plane [53].

A PLWA has a periodic cross-section and contains several periodic radiating elements, as demonstrated in Fig. 5(c).

FIGURE 10. Thinned array QLWA based on air-filled waveguide [51] ©2017 IEEE.

FIGURE 11. Conformal SIW LWA [52] ©2021 IEEE.

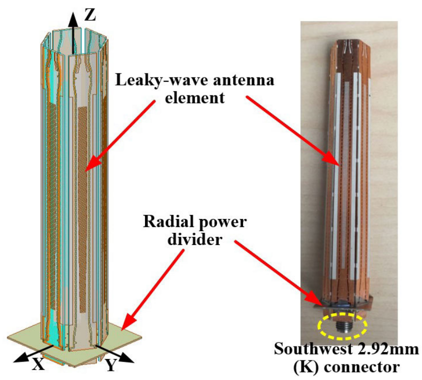

FIGURE 12. A hexangular array of SIW LWA [53] ©2020 IEEE.

Increasing the cells' period results in the excitation of higher-order Floquet modes. As a result, a PLWA can scan from backward endfire to forward endfire [1]–[5], [55]–[57]. This is one of the main advantages of a PLWA. Periodicity in the PLWA can be 1D or 2D [6], [34]. It should be mentioned that the conventional PLWAs cannot scan the broadside due to the open-stop band (OSB) phenomenon [1]–[4], [68]. The travelling wave becomes a standing wave at broadside. Hence, all the reflections add in phase, causing significant impedance mismatch. The antenna structure must be modified to enable broadside scanning. It can be done by implementing engineered structures called metamaterial cells [68]. Implementing T-Shaped slots and an array of the vias at the opposite side of transverse slots can also resolve the OSB issue, as shown in Fig. 13 [69]. Realizing LWA on a corrugated SIW and etching M-shape slots on the conducting sections averted the OSB phenomenon without using metamaterial cells, as presented in Fig. 14 [28]. Implementing sinusoidal tapered slots on the HMISW also resulted in full-space beam-scanning, as shown in Fig. 15 [19]. In microstrip-based LWA, radiation at broadside and full-space beam-scanning can be achieved by implementing cross-over strips [70] or modulated transverse slots [71], as demonstrated in Fig. 16.

III. RECONFIGURABLE LEAKY-WAVE ANTENNA

Deployment of variable links requires a beam-steerable antenna. As stated before, beam-scanning can be achieved through frequency sweep, sweeping bias voltages of

FIGURE 13. LWA with T-shaped slots and extra grounded vias [69] ©2020 IEEE.

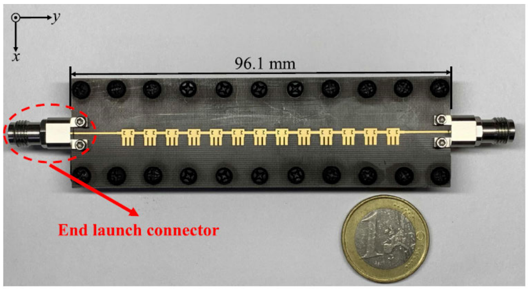

FIGURE 14. Corrugated SIW LWA with M-shaped slots [28].

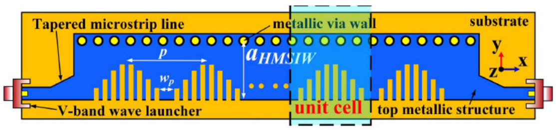

FIGURE 15. HMSIW LWA with sinusoidal periodic slots [19] ©2020 IEEE.

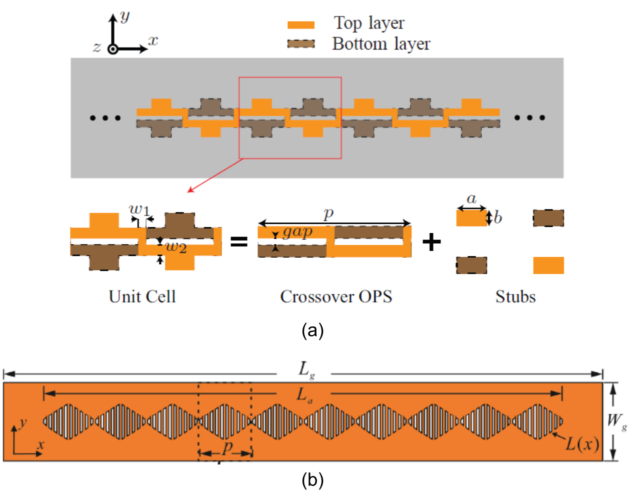

FIGURE 16. Microstrip LWA with (a) cross-over structure [70], (b) modulated transverse slots [71] ©2021 IEEE.

switches, or rotating the antenna mechanically. The electronic beam-scanning method has the broadest applications. Furthermore, using an electronic beam-scanning antenna can compensate for the unwanted frequency beam-squint in the face of variable environmental conditions. Electronic beam-scanning can be accomplished by introducing active elements such as micro-electromechanical systems (MEMS) [72]–[75], semiconductor switches, varactor diodes, PiN diodes [76], ferrite switches, or liquid crystals [76], as shown in Fig. 17. Semiconductor switches and varactor diodes have the highest switching speed and are more compact than MEMS. A varactor diode can change

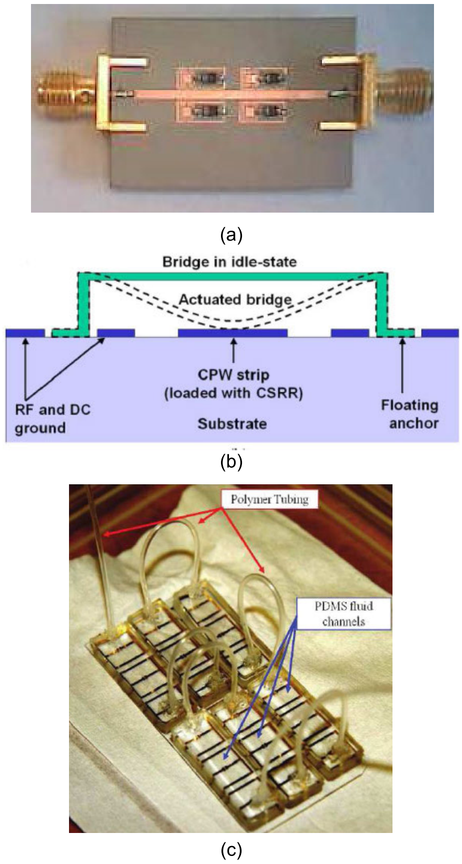

FIGURE 17. Different methods for achieving electronic beam-scanning [76] ©2015 IEEE. (a) Using switches/varactor diodes, (b) Through MEMS, (c) Implementing liquid crystal.

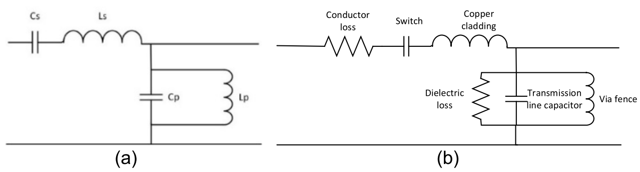

FIGURE 18. Equivalent circuit of CRLH. (a) conventional CRLH structure, (b) SIW-based CRLH structure.

the capacitance continuously by sweeping the bias voltage. A Gallium Arsenide (GaAs) varactor diode is a famous switch widely used in reconfigurable structures. Small footprint, high switching speed, ease of integration, and high packaging tolerance are among the benefits of GaAs switches. PiN diodes have the smallest footprint but provide limited switching states, i.e. "on" and "off" states. MEMS are mechanically tunable switches [72]–[75], require high bias voltage, and usually bulkier than PiN diodes and varactor diodes. However, MEMS have more comprehensive capacitance tuning ranges and often lower loss than the varactor diodes. Liquid crystals are not suitable for the integrated applications [76]. Several types of electronic beam-scanning LWAs are studied here. The investigated LWAs are microstrip- or SIW/HMSIW-based antennas.

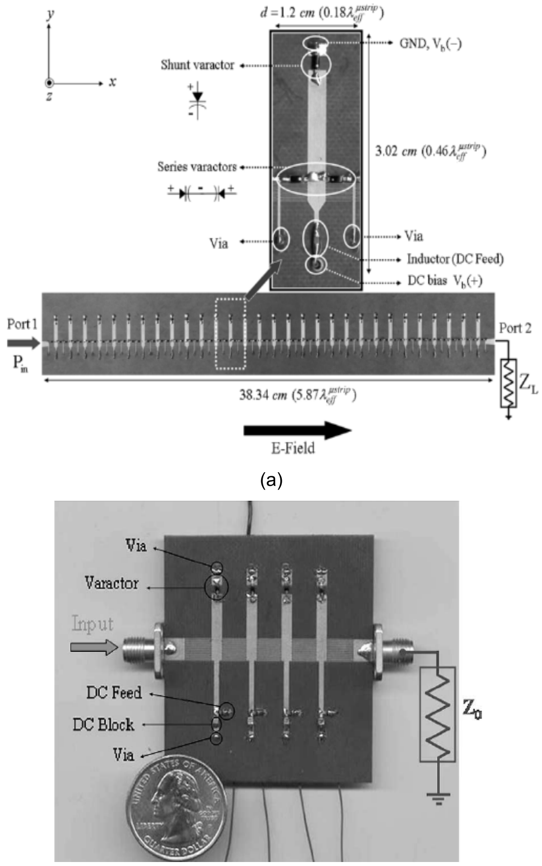

(a)

(b)

FIGURE 19. **Reconfigurable CRLH antennas with shoring stubs and interdigital capacitors. (a) fabricated antenna proposed in [91] ©2005 IEEE, (b) fabricated structure designed in [92] ©2004 IEEE, (c) radiation pattern at 18V [91], (d) radiation pattern at 2V [91].**

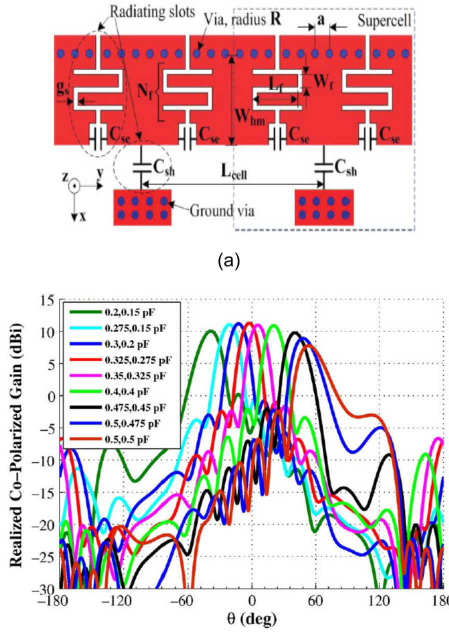

(a)

(b)

FIGURE 20. **Reconfigurable CRLH HMSIW LWA [93] ©2012 IEEE. (a) schematic of the antenna, (b) radiation pattern at 6.5 GHz.**

As stated before, according to (3), variation in β leads to θ_0 rotation and beam-steering. Variations in S-parameters, surface current, input impedance, and dielectric constant contribute to β variation and electronic beam-scanning. We categorized reconfigurable LWAs into four subgroups depending on the technology.

A. RECONFIGURABLE METAMATERIAL LWA

Reconfigurable metamaterials are widely used to achieve tunable refractive index and phase manipulation. Cloaking, tunable absorbers, tunable filters, tunable power dividers, and electronic beam-scanning antennas are among the main applications of reconfigurable metamaterials [76]. Metamaterial structures are artificially engineered to achieve unnatural responses that are difficult to achieve using conventional architectures [68]. One of the most widely applicable metamaterial structures is the composite right-hand left-hand (CRLH) structure [68], [77]–[90]. The equivalent circuit of a CRLH structure is shown in Fig. 18(a), consisting of shunt and series resonators [68]. To realize a CRLH structure, shunt inductors and series capacitors must be added to the conventional transmission line that contains shunt capacitors and series inductors [68]. In a reconfigurable HMSIW/SIW CRLH, as shown in Fig. 18(b), the top cladding, switches, substrate, and the via fences act as a series inductor, series capacitors, shunt capacitor, and shunt inductors, respectively.

The conventional structure (*i.e.,* RH structure) has positive permittivity and permeability and supports forward radiation. In contrast, the LH structure has negative permittivity and permeability and supports backward wave propagation. CRLH structure supports both backward and forward radiation depending on the frequency band. Hence, CRLH LWA scans from backward endfire to forward endfire. As stated before, implementing CRLH is a solution for overcoming the OSB issue that only happens if the balance conditions are satisfied [68], [77]–[90]. In other words, shunt and series resonance frequencies in addition to the series and shunt resonance impedance must be equal [68], [77], [78]. If the balance condition is not satisfied, a gap appears in the dispersion diagram. It should be noted that since the impedance is a function of frequency, the CRLH structure has a frequency-dependent response and the radiation at the broadside is achieved at a specific frequency band.

A CRLH structure is a suitable candidate for reconfigurable metamaterial antenna since changing CRLH cells' dimensions leads to variations in permittivity and permeability [68]. The proposed antennas in [91] and [92] were among the first reported CRLH reconfigurable LWAs, as shown in Fig. 19. Sweeping the bias voltage led to variations in the varactor diode's capacitance. This led to the variations in the impedance and propagation constant, which caused the changes in the radiation pattern. Tuning the capacitance of all varactor diodes uniformly resulted in beam-scanning, while non-uniform tuning led to variations in HPBW [92]. Both series and shunt varactor diodes were used in [92] to achieve a more flexible design approach. The antenna's beam scanned space from −49° to 50° at 3.33GHz [91] and from −10° to 7.5° at 3.23 GHz [92].

B. HMSIW-BASED RECONFIGURABLE LWA

HMSIW is a more suitable candidate for realizing a reconfigurable CRLH antenna than SIW since the shunt branches of SIW are usually not accessible [93]. A reconfigurable HHMSIW CRLH LWA was proposed in [93], as presented in Fig. 20. The proposed antenna used series and shunt tuning capacitors to achieve electronic beam-steering from −31° to 35° at 6.5 GHz with a peak gain of 9.5 dBi. In a multi-layer structure, interdigital capacitors and embedded patches can be used as series and shunt capacitors, respectively. Furthermore, the capacitors between the top cladding and grounded patches adjacent to the side aperture acted as shunt capacitors [93]. A reconfigurable HMSIW antenna with variable aperture can also be formed by placing several vias adjacent to the side aperture of HMSIW and connecting them to the aperture through sets of switches, as presented in Fig. 21 [94]. The reported antenna achieved about 80° beam-scanning range at 8.2 GHz.

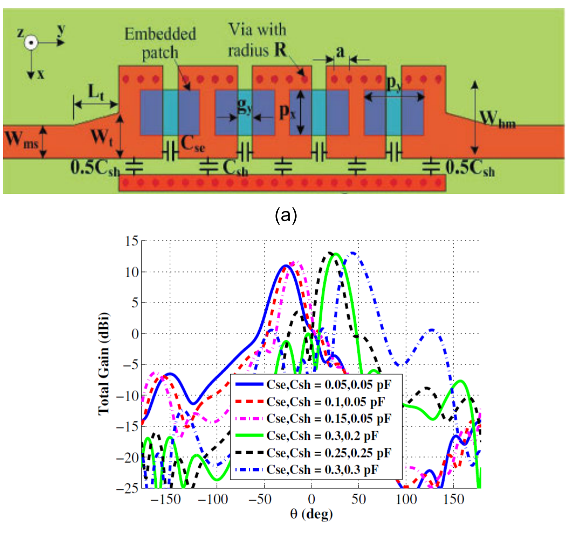

FIGURE 21. Reconfigurable CRLH HMSIW LWA with tunable grounded aperture [94] ©2011 IEEE (a) schematic of the antenna, (b) radiation pattern at 8.2 GHz.

Implementing varactor diodes on the backside of an HMSIW LWA with circular slots led to a 29° beam-scanning range with 1.2 dBi gain variation at 28.5 GHz, as illustrated in Fig. 22 [95]. It should be noted that the maximum allowable gain variation in the beam-scanning application is often 3 dBi. Considering more significant gain variation led to the over-optimistic value of the beam-scanning range. Placing RF components on the backside of the antenna resulted in the ease of fabrication and assembly. It also enhances the isolation between radiating elements and RF circuitry.

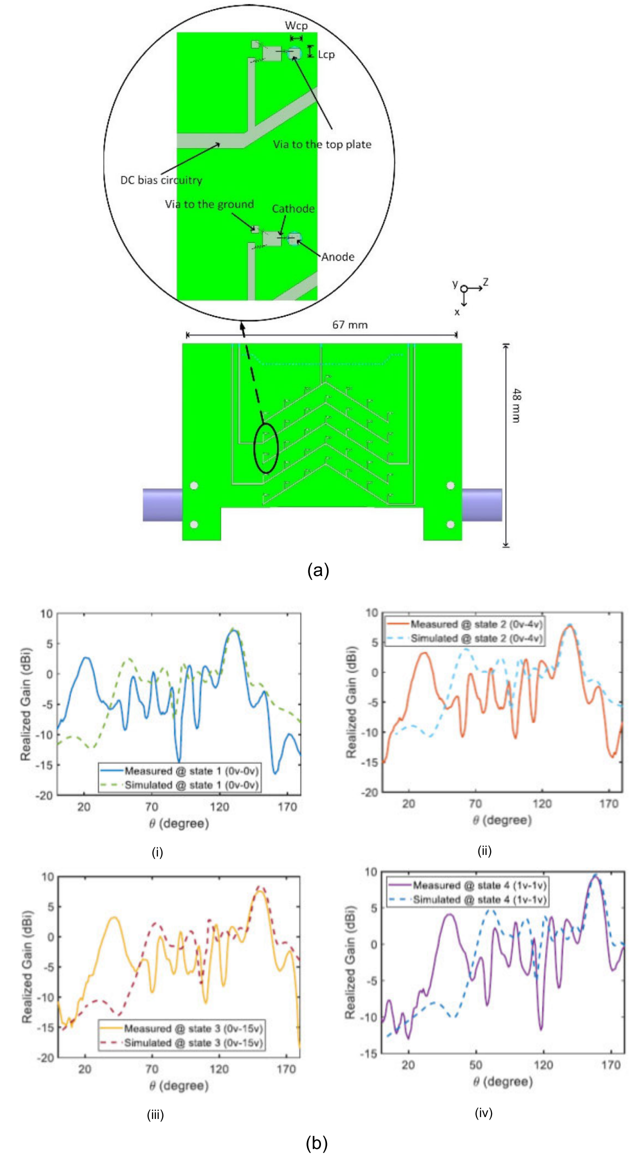

FIGURE 22. Reconfigurable HMSIW LWA with circular slots [95]. (a) The backside of the antenna, (b) radiation patterns at 28.5 GHz for different switching states.

Placing several vias near the aperture of HMSIW, creating gaps around the vias in the ground plane, and connecting the via to the ground plane through switches also led to a reconfigurable HMSIW antenna, as shown in Fig. 23 [96]. Introducing several switches over the gaps in the ground plane led to the electronic beam-scanning from 31° to 60° at 6 GHz with a peak gain of 12.9 ± 0.6 dBi [96]. It was also observed that increasing the number of reconfigurable cells resulted in a wider beam-scanning range [96]. Implementing grounded patches adjacent to the microstrip LWA in [97] resulted in a reconfigurable antenna. The reported antennas and their corresponding radiation patterns are demonstrated in Fig. 24. Switching resulted in variations in the impedance

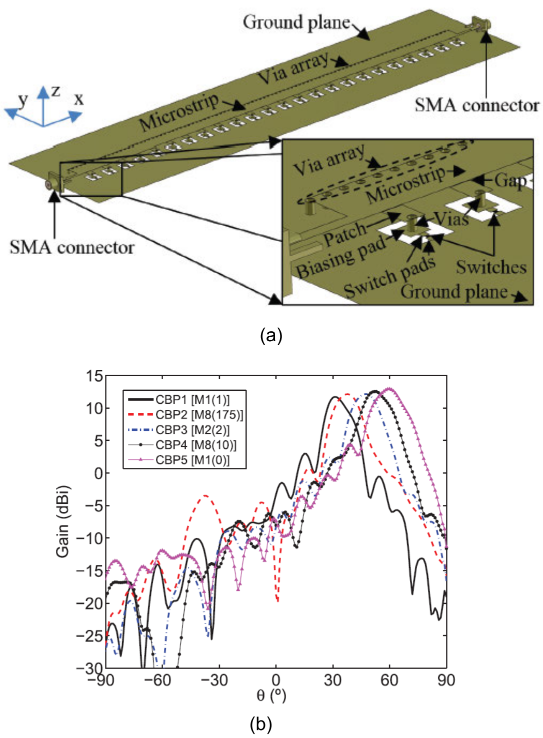

FIGURE 23. Reconfigurable HMSIW LWA with tunable grounded aperture [96] ©2016 IEEE (a) schematic of the antenna, (b) radiation pattern at 6 GHz.

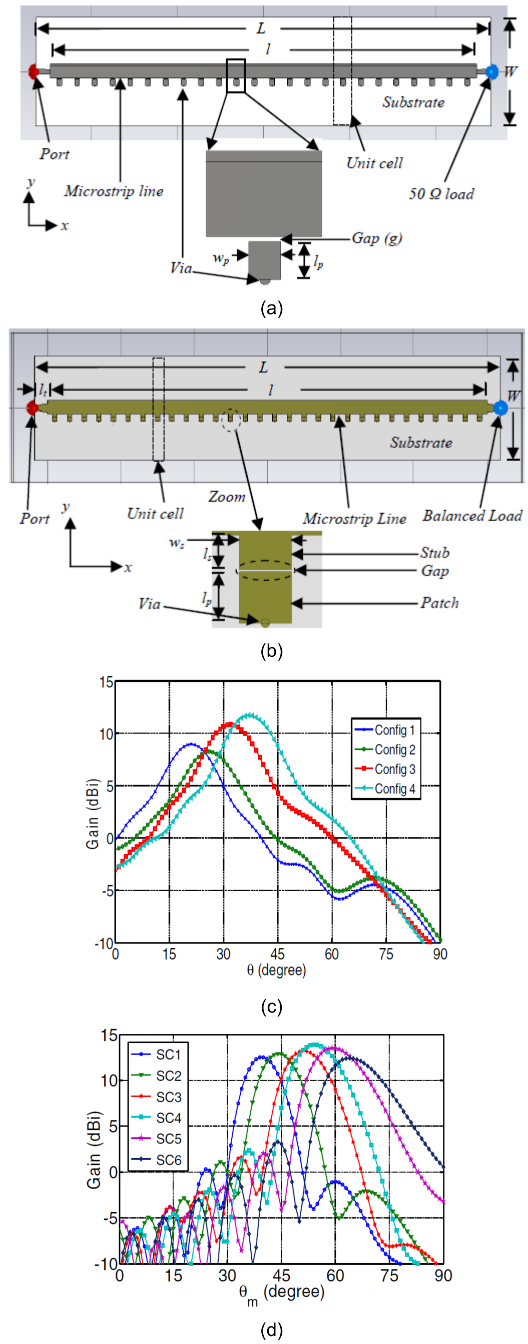

FIGURE 24. Reconfigurable microstrip antenna with periodic grounded patches (a) schematic of the antenna proposed in [97] ©2013 IEEE, (b) schematic of the antenna proposed in [98] ©2013 IEEE, (c) radiation pattern at 6.5 GHz [97], (d) radiation pattern at 6.2 GHz [98].

of each cell and the width of the top cladding. This led to the electronic beam-scanning from 21° to 37° at 6.5 GHz [97]. Similarly, loading a microstrip line with periodic grounded patches through sets of PiN diodes resulted in beam-scanning from 40° to 64° at 6.4 GHz [98].

Realizing diodes over triangular-shaped double-gap capacitors in half-width microstrip LWA resulted in forward and backward electronic beam-scanning with 1.3 dB gain variation at 4.2 GHz, as shown in Fig. 25 [99].

C. SIW-BASED RECONFIGURABLE LWA

Implementing gaps around the vias of SIW and connecting the vias to the top cladding and ground plane through PiN diodes led to a reconfigurable SIW antenna [100], [101]. Changing the diode state led to variations in the loading of the SIW and effective width. This changes the cutoff frequency and propagation constant, which led to the electric beam-scanning from 46° to 68° at 5.2 GHz, as shown in Fig. 26 [100]. Realizing sets of PiN diodes on dumbbell-shaped slots at the opposite sides in a SIW LWA, as shown in Fig. 27, leads to 125° beam-scanning at 5 GHz [102].

Implementing an array of dual-beam reconfigurable SIW LWAs provides a wide beam-scanning range at Ka-band [103]. Each LWA consists of several transverse slots, as illustrated in Fig. 28. Some of the vias were intentionally enlarged to improve radiation at the broadside by modifying the impedance. The switching was achieved by implementing three RF switch chips on the backside of the array. Using electromagnetic band-gaps (EBGs) between array elements reduced the mutual coupling as well [103].

A reconfigurable SIW LWA consists of longitudinal slots surrounded by the grounded annular ring at mm-wave is investigated in [104]. Electronic beam-scanning from −33° to 33° at 27 GHz was achieved by implementing PiN diodes

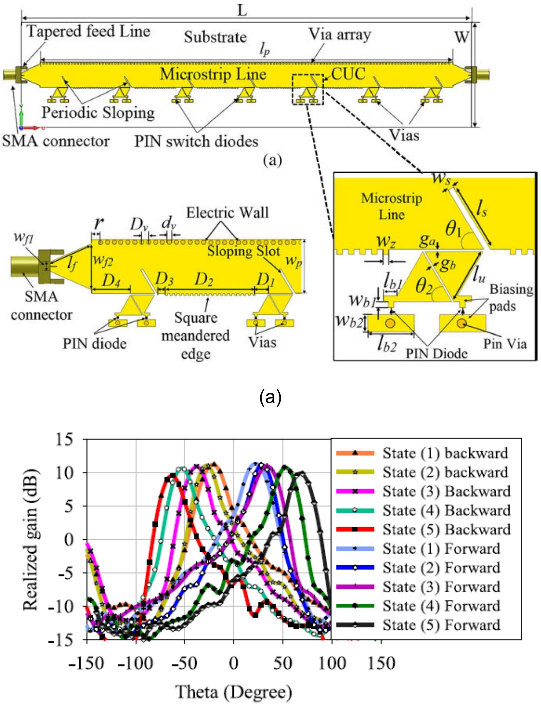

FIGURE 25. Reconfigurable microstrip LWA with triangular-shaped patches [99] ©2019 IEEE. a) Layout of the antenna, (b) Radiation pattern at 4.2 GHz.

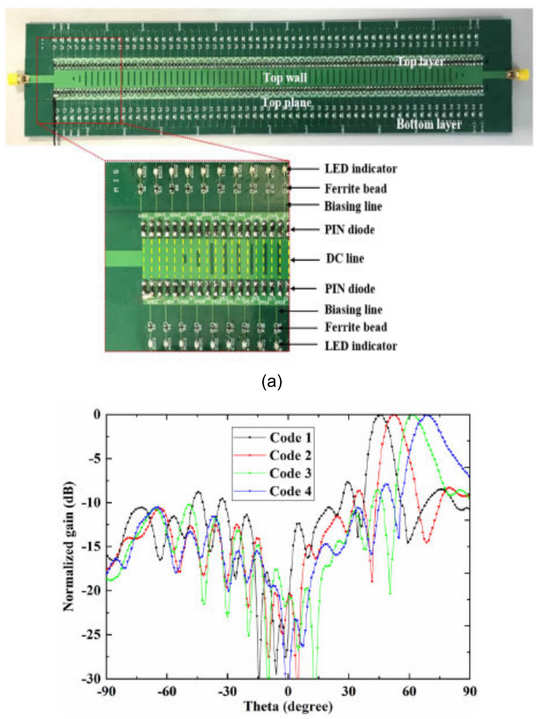

FIGURE 26. Reconfigurable SIW LWA with variable via fences [100] ©2019 IEEE. (a) schematic of the antenna, (b) radiation pattern at 5.2 GHz.

in the annular rings, as shown in Fig. 29. The slots were also fed by plated through holes [104].

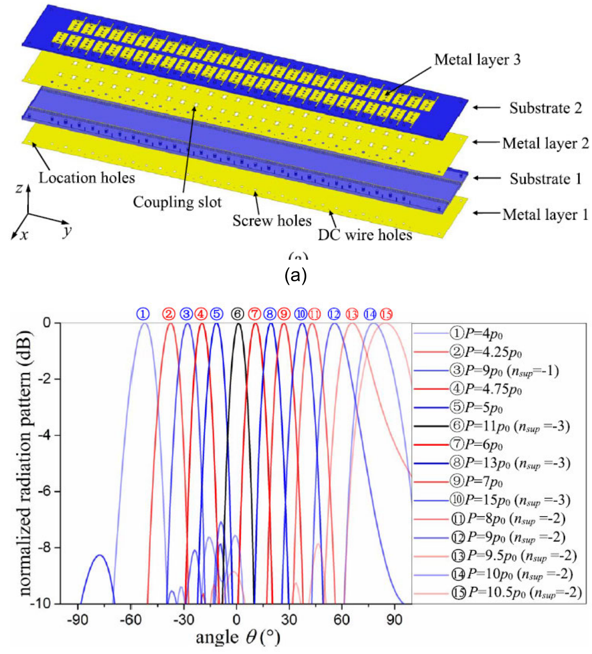

FIGURE 27. Reconfigurable SIW LWA with dumbbell-shaped slots [102] ©2019 IEEE. (a) The layout of the antenna, (b) Radiation pattern at 5 GHz.

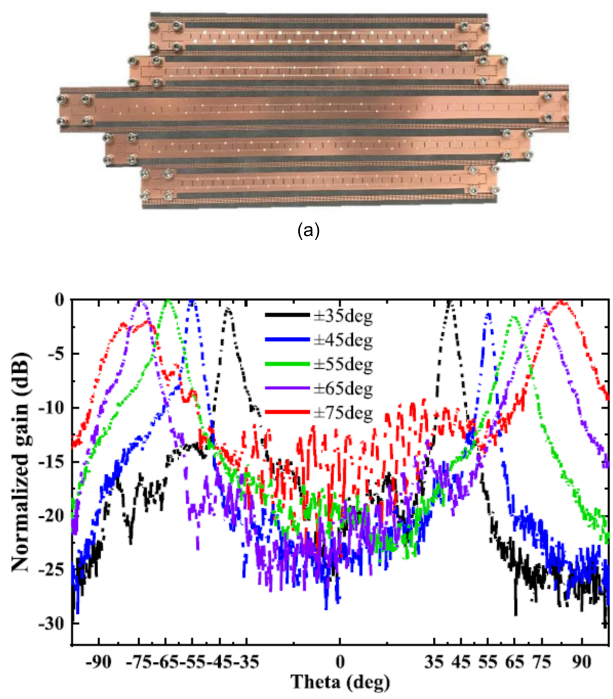

FIGURE 28. Dual-beam reconfigurable SIW LWA [103]. a) Layout of the antenna, (b) Radiation pattern at 28 GHz.

A reconfigurable corrugated SIW LWA was proposed in [105], as illustrated in Fig. 30. Corrugating the SIW helped with reducing the size of the structure. Switching the diodes led to the electric beam-scanning. The antenna scanned from 34° to 59° at 5.8 GHz with a peak gain of 12.4 dBi [105].

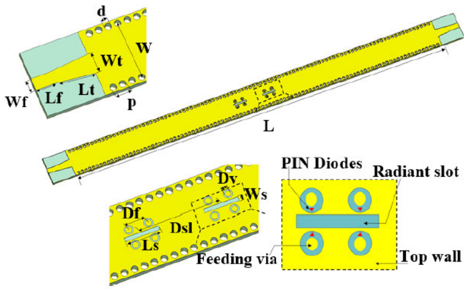

FIGURE 29. Reconfigurable SIW LWA with longitudinal slots [104].

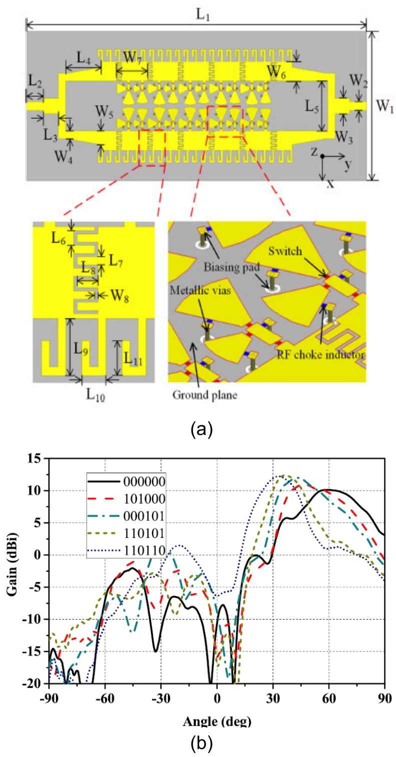

FIGURE 30. Reconfigurable corrugated SIW LWA with fan shape patches and open circuit stubs [105] ©2019 IEEE. (a) schematic of the designed antenna, (b) radiation pattern at 5.8 GHz.

Implementing sets of varactor diodes in rectangular ring slots on a corrugated SIW LWA resulted in a 72° beam-scanning range at 4.5 GHz, as shown in Fig. 31 [106].

D. MICROSTRIP-BASED RECONFIGURABLE LWA

A reconfigurable LWA achieved a 118° beam-scanning range at 8 GHz using the impedance modulation surface [107]. The electronic beam-scanning is achieved by changing the impedance of the unit cells using varactor diodes, as shown in Fig. 32 [107].

Loading a microstrip line with shunt stubs and implementing PiN diodes resulted in a 50° beam-scanning range at 2.45 GHz, as illustrated in Fig. 33 [108]. The proposed LWA has the capability of beamwidth tuning in addition to electronic beam-scanning. The beam-scanning was achieved using shunt PiN diodes by connecting/disconnecting the

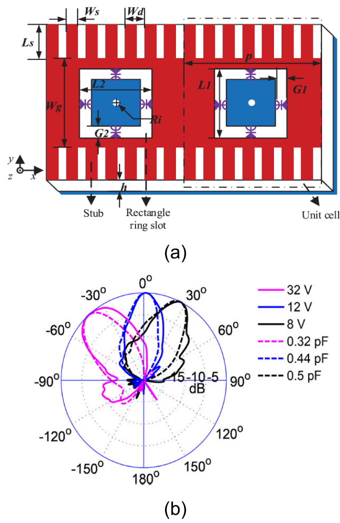

FIGURE 31. Reconfigurable corrugated SIW LWA with rectangular ring slots [106] ©2019 IEEE. (a) schematic of the antenna, (b) radiation pattern at 4.5 GHz.

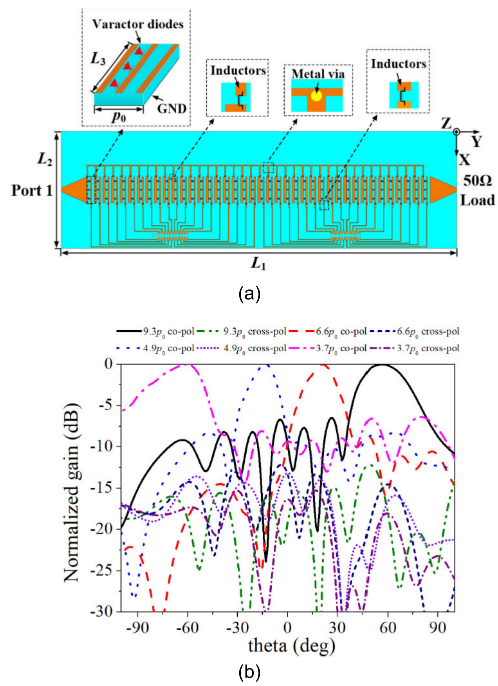

FIGURE 32. Reconfigurable LWA consists of impedance modulation surface [107] ©2020 IEEE. a) Layout of the antenna, (b) Radiation pattern at 8 GHz.

shunt stubs. At the same time, using series PiN diodes between adjacent cells led to beamwidth tuning [108].

A reconfigurable microstrip LWA was introduced in [109], including a staggered-shaped strip line and periodic longitudinal patches adjacent to it, as shown in Fig. 34. Introducing sets of switches led to the variation in the surface current, which resulted in electronic beam scanning from 60° to 135° at 4.5 GHz [109].

All the above-mentioned LWAs have pattern reconfigurability and electronic beam-scanning antenna. It is also

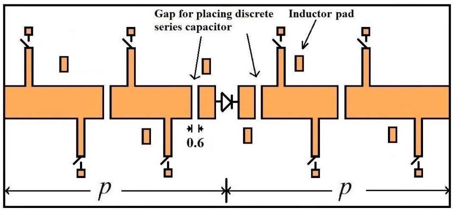

FIGURE 33. Reconfigurable microstrip LWA with series and shunt PiN diodes [108] ©2020 IEEE.

FIGURE 34. Reconfigurable microstrip LWA with a staggered strip line [109].

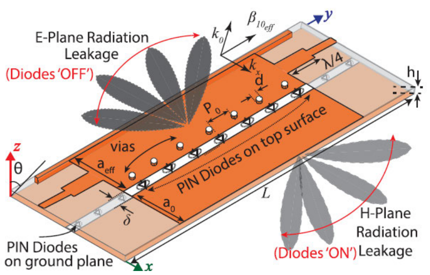

FIGURE 35. SIW LWA with switchable patterns [111].

possible to achieve polarization adaptivity by connecting/disconnecting shorted stubs using PiN diodes, as reported in [110]. Moreover, it is possible to switch radiation patterns between E- and H-planes by placing sets of PiN diodes on the gapped SIW LWA, as shown in Fig. 35 [111].

IV. COMPARISON BETWEEN RECONFIGURABLE LEAKY-WAVE ANTENNAS

A comparison among the investigated reconfigurable LWAs has been made and reported in Table 1. The reported antennas in [102] and [107] have the widest beam-scanning range with a relatively small gain variation. The investigated antennas in [96], [98], and [103] radiate with the highest gain. In comparison, [92] and [106] have the smallest gain variation. The investigated antennas in [92] and [94] are the most compact ones as well. Overall, the proposed antennas in [94], [102], and [109] are the most suitable ones for the miniaturized beam-scanning applications due to their wide beam-scanning range, high gain, small gain variation, and compactness.

It should be noted that the reported LWAs in [91]–[94], [96]–[102], and [105]–[109] are not operating in the mm-wave frequency band and not suitable for mm-wave beam-scanning applications. Furthermore, the reported antennas in [91], [92], [96]–[99], and [107]–[109] are microstrip-based LWAs, while [93]–[95], [100], and [102]–[106] are SIW/HMSIW-based LWAs. Hence [91], [92], [96]–[99], and [107]–[109] are more affordable because punching via holes and filling them with conductive epoxy often increase the fabrication cost of SIW/HMSIW-based antennas. However, as stated before, SIW/HMSIW-based LWAs are easier and cheaper to fabricate than the ones based on metallic waveguides and gap waveguides. The reported LWAs in [93] and [94] use series and shunt switches, adding to the design's complexity.

TABLE 1. Comparison among the investigated reconfigurable LWAs.

Reference	Antenna Length	Center Frequency	Beam-Scanning Range	Gain
[91]	5.87 × λ	3.33 GHz	99°	8 ± 10 dBi
[92]	0.75 × λ	3.23 GHz	17.5°	-5.8 ± 0.25 dBi
[93]	3.25 × λ	6.5 GHz	66°	10 ± 1 dBi
[94]	0.52 × λ	8.2 GHz	80°	12 ± 1 dBi
[95]	3.7 × λ	28.5 GHz	29°	8.2 ± 0.6 dBi
[96]	5.32 × λ	6 GHz	29°	12.9 ± 0.6 dBi
[97]	5.35 × λ	6.5 GHz	16°	10 ± 2 dBi
[98]	6.57 × λ	6.4 GHz	24°	13 ± 1 dBi
[99]	3 × λ	4.2 GHz	38°	11.12 ± 0.65 dBi
[100]	6.11 × λ	5.2 GHz	22°	4 ± 1.5 dBi
[102]	4.6 × λ	5 GHz	125°	11.8 ± 1.5 dBi
[103]	24.3 × λ	28 GHz	40 °	14 ± 1 dBi
[104]	9 × λ	27 GHz	66°	5.5 ± 1.5 dBi
[105]	3.83 × λ	5.8 GHz	25°	11.2 ± 1.2 dBi
[106]	3.6 × λ	4.5 GHz	72°	5.6 ± 0.3 dBi
[107]	4.3 × λ	8 GHz	118°	8.2 ± 1.25 dBi
[108]	2.29 × λ	2.45 GHz	50°	7.5 ± 0.6 dBi
[109]	4.2 × λ	4.5 GHz	76°	9 ± 1 dBi

V. CONCLUSION

In this paper, a comprehensive review of reconfigurable LWAs was performed to guide the LWA designers. First, the basic concepts of LWA were studied. Therefore, beam-scanning mechanism, guiding structures, and different types of LWAs were investigated thoroughly. Then the state-of-the-art frequency and electronic beam-scanning LWAs were investigated to highlight viable options in response to the challenges of LWAs. Next, a comparison between several reconfigurable LWAs was performed from different aspects, such as size, frequency band, beam-scanning range, and gain. Overall, relatively wide beam-scanning range, high gain, compactness, simplicity of the feed network, and ease of fabrication make reconfigurable LWAs suitable candidates for beam-scanning applications. Reducing the gain variations by beam-scanning, tuning beamwidth independent of the main-lobe pointing angle, and increasing the radiation efficiency are among the current challenges of LWA, which require further investigations.

REFERENCES

[1] J. L. Volakis, *Antenna Engineering Handbook*, 4th ed. New York, NY, USA: McGraw-Hill, 2007.

[2] C. A. Balanis, *Modern Antenna Handbook*, 1st ed. New York, NY, USA: Wiley, 2008.

[3] D. R. Jackson, C. Caloz, and T. Itoh, "Leaky-wave antennas," *Proc. IEEE*, vol. 100, no. 7, pp. 2194–2206, Jul. 2012.

[4] F. Monticone and A. Alu, "Leaky-wave theory, techniques, and applications: From microwaves to visible frequencies," *Proc. IEEE*, vol. 103, no. 5, pp. 793–821, May 2015.

[5] F. B. Gross, *Frontiers in Antennas: Next Generation Design and Engineering*, 1st ed. New York, NY, USA: McGraw-Hill, 2011.

[6] F. Xu and K. Wu, "Guided-wave and leakage characteristics of substrate integrated waveguide," *IEEE Trans. Microw. Theory Techn.*, vol. 53, no. 1, pp. 66–73, Jan. 2005.

[7] M. Bozzi, A. Georgiadis, and K. Wu, "Review of substrate integrated waveguide circuits and antennas," *IET Microw., Antennas Propag.*, vol. 5, no. 8, pp. 909–920, 2011.

[8] J. Liu and J. Liang, "Gain enhancement of transversely-slotted substrate integrated waveguide leaky-wave antennas based on higher modes," *IEEE Trans. Antennas Propag.*, early access, Jan. 8, 2021, doi: 10.1109/TAP.2020.3048597.

[9] Y. Mohtashami and J. Rashed-Mohassel, "A butterfly substrate integrated waveguide leaky-wave antenna," *IEEE Trans. Antennas Propag.*, vol. 62, no. 6, pp. 3384–3388, Jun. 2014.

[10] J. Xu, W. Hong, H. Tang, Z. Kuai, and K. Wu, "Half-mode substrate integrated waveguide (HMSIW) leaky-wave antenna for millimeter-wave applications," *IEEE Antennas Wireless Propag. Lett.*, vol. 7, pp. 85–88, 2008.

[11] Q. Lai, C. Fumeaux, W. Hong, and R. Vahldieck, "Characterization of the propagation properties of the half-mode substrate integrated waveguide," *IEEE Trans. Microw. Theory Techn.*, vol. 57, no. 8, pp. 1996–2004, Aug. 2009.

[12] N. Nguyen-Trong, T. Kaufmann, and C. Fumeaux, "A wideband omnidirectional horizontally polarized traveling-wave antenna based on half-mode substrate integrated waveguide," *IEEE Antennas Wireless Propag. Lett.*, vol. 12, pp. 682–685, 2013.

[13] N. Nguyen-Trong, T. Kaufmann, and C. Fumeaux, "A semi-analytical solution of a tapered half-mode substrate-integrated waveguide with application to rapid antenna optimization," *IEEE Trans. Antennas Propag.*, vol. 62, no. 6, pp. 3189–3200, Jun. 2014.

[14] N. Nguyen-Trong, L. Hall, and C. Fumeaux, "Transmission-line model of nonuniform leaky-wave antennas," *IEEE Trans. Antennas Propag.*, vol. 64, no. 3, pp. 883–893, Mar. 2016.

[15] N. Javanbakht, R. E. Amaya, J. Shaker, and B. Syrett, "Side-lobe level reduction of half-mode substrate integrated waveguide leaky-wave antenna," *IEEE Trans. Antennas Propag.*, vol. 69, no. 6, pp. 3572–3577, Jun. 2021.

[16] X. Zou, C. Tong, H. He, and F. Geng, "Edge-radiating slot antenna based on half-mode substrate integrated waveguide," *IET Microw., Antennas Propag.*, vol. 11, no. 8, pp. 1106–1112, Jun. 2017.

[17] K. Y. Kapusuz, A. V. Berghe, S. Lemey, and H. Rogier, "Partially filled half-mode substrate integrated waveguide leaky-wave antenna for 24 GHz automotive radar," *IEEE Antennas Wireless Propag. Lett.*, vol. 20, no. 1, pp. 33–37, Jan. 2021.

[18] X. Chen, Z. Li, H. Song, and J. Wang, "Generation of radiation null for the HMSIW leaky-wave antenna," *IEEE Antennas Wireless Propag. Lett.*, vol. 16, pp. 2688–2691, 2017.

[19] A. Sarkar and S. Lim, "60 GHz compact larger beam scanning range PCB leaky-wave antenna using HMSIW for millimeter-wave applications," *IEEE Trans. Antennas Propag.*, vol. 68, no. 8, pp. 5816–5826, Aug. 2020.

[20] S. van Berkel, E. S. Malotaux, C. De Martino, M. Spirito, D. Cavallo, A. Neto, and N. Llombart, "Wideband double leaky slot lens antennas in CMOS technology at submillimeter wavelengths," *IEEE Trans. THz Sci. Technol.*, vol. 10, no. 5, pp. 540–553, Sep. 2020.

[21] U. Dey, J. Tonn, and J. Hesselbarth, "Millimeter-wave dielectric waveguide-based leaky-wave antenna array," *IEEE Antennas Wireless Propag. Lett.*, vol. 20, no. 3, pp. 361–365, Mar. 2021.

[22] A. Zandamela, A. Al-Bassam, and D. Heberling, "Circularly polarized periodic leaky-wave antenna based on dielectric image line for millimeter-wave radar applications," *IEEE Antennas Wireless Propag. Lett.*, vol. 20, no. 6, pp. 938–942, Jun. 2021.

[23] A. Attar and A. R. Sebak, "High gain periodic 2-D leaky-wave antenna with backward radiation for millimeter-wave band," *IEEE Open J. Antennas Propag.*, vol. 2, pp. 49–61, 2021.

[24] J. Chen, W. Yuan, W. X. Tang, L. Wang, Q. Cheng, and T. J. Cui, "Linearly sweeping leaky-wave antenna with high scanning rate," *IEEE Trans. Antennas Propag.*, vol. 69, no. 6, pp. 3214–3223, Jun. 2021.

[25] Y. F. Wu, Y. J. Cheng, S. S. Yao, and Y. Fan, "Millimeter-wave near-field-focused full 2-D frequency scanning antenna array with height-modulated-ridge waveguide," *IEEE Trans. Antennas Propag.*, vol. 69, no. 5, pp. 2595–2604, May 2021.

[26] S. Wang, Z. Li, B. Wei, S. Liu, and J. Wang, "A Ka-band circularly polarized fixed-frequency beam-scanning leaky-wave antenna based on groove gap waveguide with consistent high gains," *IEEE Trans. Antennas Propag.*, vol. 69, no. 4, pp. 1959–1969, Apr. 2021.

[27] J. Cao, H. Wang, S. Tao, S. Mou, and Y. Guo, "Highly integrated beam scanning groove gap waveguide leaky wave antenna array," *IEEE Trans. Antennas Propag.*, early access, May 25, 2020, doi: 10.1109/TAP.2020.2995470.

[28] Y. Zhang, H. Liu, C. Meng, Y. Lin, Y. Zhang, E. Forsberg, and S. He, "A broadband high-gain circularly polarized wide beam scanning leaky-wave antenna," *IEEE Access*, vol. 8, pp. 171091–171099, 2020.

[29] D. Zheng and K. Wu, "Multifunctional filtering leaky-wave antenna exhibiting simultaneous rapid beam-scanning and frequency-selective characteristics based on radiative bandpass filter concept," *IEEE Trans. Antennas Propag.*, vol. 68, no. 8, pp. 5842–5854, Aug. 2020.

[30] M. K. Emara and S. Gupta, "Integrated multi-port leaky-wave antenna multiplexer/demultiplexer system for millimeter-wave communication," *IEEE Trans. Antennas Propag.*, early access, Feb. 24, 2021, doi: 10.1109/TAP.2021.3060138.

[31] Q. Liao and L. Wang, "Switchable bidirectional/unidirectional LWA array based on half-mode substrate integrated waveguide," *IEEE Antennas Wireless Propag. Lett.*, vol. 19, no. 7, pp. 1261–1265, Jul. 2020.

[32] M. Agiwal, A. Roy, and N. Saxena, "Next generation 5G wireless networks: A comprehensive survey," *IEEE Commun. Surveys Tuts.*, vol. 18, no. 3, pp. 1617–1655, 3rd Quart., 2016.

[33] B. Cao, H. Wang, Y. Huang, and J. Zheng, "High-gain L-probe excited substrate integrated cavity antenna array with LTCC-based gap waveguide feeding network for W-band application," *IEEE Trans. Antennas Propag.*, vol. 63, no. 12, pp. 5465–5474, Dec. 2015.

[34] F. F. Manzillo, M. Ettorre, M. S. Lahti, K. T. Kautio, D. Lelaidier, E. Seguenot, and R. Sauleau, "A multilayer LTCC solution for integrating 5G access point antenna modules," *IEEE Trans. Microw. Theory Techn.*, vol. 64, no. 7, pp. 2272–2283, Jul. 2016.

[35] Z. L. Ma, L. J. Jiang, S. Gupta, and W. E. I. Sha, "Dispersion characteristics analysis of one dimensional multiple periodic structures and their applications to antennas," *IEEE Trans. Antennas Propag.*, vol. 63, no. 1, pp. 113–121, Jan. 2015.

[36] J. Liu, D. R. Jackson, and Y. Long, "Modal analysis of dielectric-filled rectangular waveguide with transverse slots," *IEEE Trans. Antennas Propag.*, vol. 59, no. 9, pp. 3194–3203, Sep. 2011.

[37] M. Z. Ali and Q. U. Khan, "High gain backward scanning substrate integrated waveguide leaky wave antenna," *IEEE Trans. Antennas Propag.*, vol. 69, no. 1, pp. 562–565, Jan. 2021.

[38] M. R. Rahimi, M. S. Sharawi, and K. Wu, "Higher-order space harmonics in substrate integrated waveguide leaky-wave antennas," *IEEE Trans. Antennas Propag.*, early access, Jan. 8, 2021, doi: 10.1109/TAP.2020.3048530.

[39] Y.-W. Wu, Z. Jiang, and Z.-C. Hao, "A 400-GHz low cost planar leaky-wave antenna with low sidelobe level and low cross-polarization level," *IEEE Trans. THz Sci. Technol.*, vol. 10, no. 4, pp. 427–430, Jul. 2020.

[40] L. Sun, P. Liu, Y. Li, L. Chang, K. Wei, and Z. Zhang, "Metal strip endfire antenna based on TE1 leaky-wave mode," *IEEE Trans. Antennas Propag.*, vol. 68, no. 8, pp. 5916–5923, Aug. 2020.

[41] Z. Kordiboroujeni and J. Bornemann, "Designing the width of substrate integrated waveguide structures," *IEEE Microw. Wireless Compon. Lett.*, vol. 23, no. 10, pp. 518–520, Oct. 2013.

[42] Y. Cassivi, L. Perregrini, P. Arcioni, M. Bressan, K. Wu, and G. Conciauro, "Dispersion characteristics of substrate integrated rectangular waveguide," *IEEE Microw. Wireless Compon. Lett.*, vol. 12, no. 9, pp. 333–335, Sep. 2002.

[43] D. Deslandes and K. Wu, "Accurate modeling, wave mechanisms, and design considerations of a substrate integrated waveguide," *IEEE Trans. Microw. Theory Techn.*, vol. 54, no. 6, pp. 2516–2526, Jun. 2006.

[44] M. Salehi and E. Mehrshahi, "A closed-form formula for dispersion characteristics of fundamental SIW mode," *IEEE Microw. Wireless Compon. Lett.*, vol. 21, no. 1, pp. 4–6, Jan. 2011.

[45] Y. J. Cheng, W. Hong, K. Wu, and Y. Fan, "Millimeter-wave substrate integrated waveguide long slot leaky-wave antennas and two-dimensional multibeam applications," *IEEE Trans. Antennas Propag.*, vol. 59, no. 1, pp. 40–47, Jan. 2011.

[46] D. Zheng, Y.-L. Lyu, and K. Wu, "Longitudinally slotted SIW leaky-wave antenna for low cross-polarization millimeter-wave applications," *IEEE Trans. Antennas Propag.*, vol. 68, no. 2, pp. 656–664, Feb. 2020.

[47] A. M. Malekshah, M. S. Majedi, and A. R. Attari, "Improved design of a SIW long slot leaky wave antenna with low SLL," *IET Microw., Antennas Propag.*, vol. 13, no. 1, pp. 112–117, Jan. 2019.

[48] A. M. Malekshah, A. R. Attari, and M. S. Majedi, "Improved design of uniform SIW leaky wave antenna by considering the unwanted mode," *IEEE Trans. Antennas Propag.*, vol. 68, no. 8, pp. 6378–6382, Aug. 2020.

[49] J. Liu, D. R. Jackson, and Y. Long, "Substrate integrated waveguide (SIW) leaky-wave antenna with transverse slots," *IEEE Trans. Antennas Propag.*, vol. 60, no. 1, pp. 20–29, Jan. 2012.

[50] J. Liu, D. R. Jackson, Y. Li, C. Zhang, and Y. Long, "Investigations of SIW leaky-wave antenna for endfire-radiation with narrow beam and sidelobe suppression," *IEEE Trans. Antennas Propag.*, vol. 62, no. 9, pp. 4489–4497, Sep. 2014.

[51] N. Javanbakht, M. S. Majedi, and A. R. Attari, "Thinned array inspired quasi-uniform leaky-wave antenna with low side-lobe level," *IEEE Antennas Wireless Propag. Lett.*, vol. 16, pp. 2992–2995, 2017.

[52] E. Çelenk and N. T. Tokan, "Frequency scanning conformal sensor based on SIW metamaterial antenna," *IEEE Sensors J.*, early access, Apr. 26, 2021, doi: 10.1109/JSEN.2021.3075556.

[53] D. Zheng, Y.-L. Lyu, and K. Wu, "Transversely slotted SIW leaky-wave antenna featuring rapid beam-scanning for millimeter-wave applications," *IEEE Trans. Antennas Propag.*, vol. 68, no. 6, pp. 4172–4185, Jun. 2020.

[54] Q. Zhang, Q. Zhang, H. Liu, and C. H. Chan, "Dual-band and dual-polarized leaky-wave antenna based on slotted SIW," *IEEE Antennas Wireless Propag. Lett.*, vol. 18, no. 3, pp. 507–511, Mar. 2019.

[55] S. Sengupta, D. R. Jackson, A. T. Almutawa, H. Kazemi, F. Capolino, and S. A. Long, "A cross-shaped 2-D periodic leaky-wave antenna," *IEEE Trans. Antennas Propag.*, vol. 68, no. 3, pp. 1289–1301, Mar. 2020.

[56] D. K. Karmokar, Y. J. Guo, P.-Y. Qin, S.-L. Chen, and T. S. Bird, "Substrate integrated waveguide-based periodic backward-to-forward scanning leaky-wave antenna with low cross-polarization," *IEEE Trans. Antennas Propag.*, vol. 66, no. 8, pp. 3846–3856, Aug. 2018.

[57] S.-L. Chen, D. K. Karmokar, Z. Li, P.-Y. Qin, R. W. Ziolkowski, and Y. J. Guo, "Circular-polarized substrate-integrated-waveguide leaky-wave antenna with wide-angle and consistent-gain continuous beam scanning," *IEEE Trans. Antennas Propag.*, vol. 67, no. 7, pp. 4418–4428, Jul. 2019.

[58] Y. Geng, J. Wang, Z. Li, Y. Li, M. Chen, and Z. Zhang, "Dual-beam and tri-band SIW leaky-wave antenna with wide beam scanning range including broadside direction," *IEEE Access*, vol. 7, pp. 176361–176368, 2019.

[59] Y.-L. Lyu, X.-X. Liu, P.-Y. Wang, D. Erni, Q. Wu, C. Wang, N.-Y. Kim, and F.-Y. Meng, "Leaky-wave antennas based on noncutoff substrate integrated waveguide supporting beam scanning from backward to forward," *IEEE Trans. Antennas Propag.*, vol. 64, no. 6, pp. 2155–2164, Jun. 2016.

[60] N. Javanbakht, R. E. Amaya, J. Shaker, and B. Syrett, "A tapered CPW fed leaky-wave antenna based on substrate integrated waveguide with reduced side-lobe level," *Int. J. RF Microw. Comput.-Aided Eng.*, vol. 31, no. 5, Feb. 2021, Art. no. e22607.

[61] P. Luo, W. He, Y. Zhang, H. Liu, E. Forsberg, and S. He, "Leaky-wave antenna with wide scanning range based on double-layer substrate integrated waveguide," *IEEE Access*, vol. 8, pp. 199899–199908, 2020.

[62] H. Uchimura, T. Takenoshita, and M. Fujii, "Development of a 'laminated waveguide,"' *IEEE Trans. Microw. Theory Techn.*, vol. 46, no. 12, pp. 2438–2443, Dec. 1998.

[63] J. Hirokawa and M. Ando, "Single-layer feed waveguide consisting of posts for plane TEM wave excitation in parallel plates," *IEEE Trans. Antennas Propag.*, vol. 46, no. 5, pp. 625–630, May 1998.

[64] D. Deslandes and K. Wu, "Integrated microstrip and rectangular waveguide in planar form," *IEEE Microw. Wireless Compon. Lett.*, vol. 11, no. 2, pp. 68–70, Feb. 2001.

[65] D. M. Pozar, *Microwave Engineering*, 3rd ed. New York, NY, USA: Wiley, 2005.

[66] C. A. Balanis, *Advanced Engineering Electromagnetics*, 2nd ed. New York, NY, USA: Wiley, 2012.

[67] F. Mesa and D. R. Jackson, "The danger of high-frequency spurious effects on wide microstrip line," *IEEE Trans. Microw. Theory Techn.*, vol. 50, no. 12, pp. 2679–2689, Dec. 2002.

[68] C. Caloz and T. Itoh, *Electromagnetic Metamaterials: Transmission Line Theory and Microwave Applications*, 1st ed. Hoboken, NJ, USA: Wiley, 2005.

[69] D. K. Karmokar, S.-L. Chen, D. Thalakotuna, P.-Y. Qin, T. S. Bird, and Y. J. Guo, "Continuous backward-to-forward scanning 1-D slot-array leaky-wave antenna with improved gain," *IEEE Antennas Wireless Propag. Lett.*, vol. 19, no. 1, pp. 89–93, Jan. 2020.

[70] S. Ge, Q. Zhang, A. K. Rashid, Y. Zhang, H. Wang, and R. Murch, "A compact full-space scanning leaky-wave antenna with stable peak gains," *IEEE Trans. Antennas Propag.*, early access, May 13, 2021, doi: 10.1109/TAP.2021.3078242.

[71] J. Liu, "Periodic leaky-wave antennas based on microstrip-fed slot array with different profile modulations for suppressing open stopband and $n = -2$ space harmonic," *IEEE Trans. Antennas Propag.*, early access, May 14, 2021, doi: 10.1109/TAP.2021.3078525.

[72] T. Zvolensky, D. Chicherin, A. V. Räisänen, and C. Simovski, "Leaky-wave antenna based on micro-electromechanical systems-loaded microstrip line," *IET Microw., Antennas Propag.*, vol. 5, no. 3, pp. 357–363, 2011.

[73] E. Erdil, K. Topalli, M. Unlu, O. A. Civi, and T. Akin, "Frequency tunable microstrip patch antenna using RF MEMS technology," *IEEE Trans. Antennas Propag.*, vol. 55, no. 4, pp. 1193–1196, Apr. 2007.

[74] L.-Y. Ma, N. Soin, M. H. M. Daut, and S. F. W. M. Hatta, "Comprehensive study on RF-MEMS switches used for 5G scenario," *IEEE Access*, vol. 7, pp. 107506–107522, 2019.

[75] T. Hand and S. Cummer, "Characterization of tunable metamaterial elements using MEMS switches," *IEEE Antennas Wireless Propag. Lett.*, vol. 6, pp. 401–404, 2007.

[76] G. Oliveri, D. H. Werner, and A. Massa, "Reconfigurable electromagnetics through metamaterials—A review," *Proc. IEEE*, vol. 103, no. 7, pp. 1034–1056, Jul. 2015.

[77] C. Caloz, "Metamaterial dispersion engineering concepts and applications," *Proc. IEEE*, vol. 99, no. 10, pp. 1711–1719, Oct. 2011.

[78] M. R. M. Hashemi and T. Itoh, "Evolution of composite right/left-handed leaky-wave antennas," *Proc. IEEE*, vol. 99, no. 10, pp. 1746–1754, Oct. 2011.

[79] S. Otto, A. Rennings, K. Solbach, and C. Caloz, "Transmission line modeling and asymptotic formulas for periodic leaky-wave antennas scanning through broadside," *IEEE Trans. Antennas Propag.*, vol. 59, no. 10, pp. 3695–3709, Oct. 2011.

[80] S. Otto, A. Al-Bassam, A. Rennings, K. Solbach, and C. Caloz, "Radiation efficiency of longitudinally symmetric and asymmetric periodic leaky-wave antennas," *IEEE Antennas Wireless Propag. Lett.*, vol. 11, pp. 612–615, 2012.

[81] S. Otto, A. Al-Bassam, A. Rennings, K. Solbach, and C. Caloz, "Transversal asymmetry in periodic leaky-wave antennas for bloch impedance and radiation efficiency equalization through broadside," *IEEE Trans. Antennas Propag.*, vol. 62, no. 10, pp. 5037–5054, Oct. 2014.
[82] D. K. Karmokar, Y. J. Guo, S.-L. Chen, and T. S. Bird, "Composite right/left-handed leaky-wave antennas for wide-angle beam scanning with flexibly chosen frequency range," *IEEE Trans. Antennas Propag.*, vol. 68, no. 1, pp. 100–110, Jan. 2020.
[83] Y. Dong and T. Itoh, "Composite right/left-handed substrate integrated waveguide and half mode substrate integrated waveguide leaky-wave structures," *IEEE Trans. Antennas Propag.*, vol. 59, no. 3, pp. 767–775, Mar. 2011.
[84] M. M. Sabahi, A. A. Heidari, and M. Movahhedi, "A compact CRLH circularly polarized leaky-wave antenna based on substrate-integrated waveguide," *IEEE Trans. Antennas Propag.*, vol. 66, no. 9, pp. 4407–4414, Sep. 2018.
[85] F. P. Casares-Miranda, C. Camacho-Peñalosa, and C. Caloz, "High-gain active composite right/left-handed leaky-wave antenna," *IEEE Trans. Antennas Propag.*, vol. 54, no. 8, pp. 2292–2300, Aug. 2006.
[86] S. S. Haghighi, A.-A. Heidari, and M. Movahhedi, "A three-band substrate integrated waveguide leaky-wave antenna based on composite right/left-handed structure," *IEEE Trans. Antennas Propag.*, vol. 63, no. 10, pp. 4578–4582, Oct. 2015.
[87] M. Alibakhshikenari, B. S. Virdee, C. H. See, R. A. Abd-Alhameed, F. Falcone, and E. Limiti, "High-isolation leaky-wave array antenna based on CRLH metamaterial implemented on SIW with ±30° frequency beam-scanning capability at millimeter-waves," *Electronics*, vol. 8, no. 6, pp. 642–657, 2019.
[88] M. Alibakhshikenari, B. S. Virdee, M. Khalily, P. Shukla, C. H. See, R. A. Abd-Alhameed, F. Falcone, and E. Limiti, "Beam-scanning leaky-wave antenna based on CRLH-metamaterial for millimeter-wave applications," *IET Microw., Antennas Propag.* vol. 13, no. 8, pp. 1129–1133, Jul. 2019.
[89] D. K. Karmokar, Y. J. Guo, S.-L. Chen, and T. S. Bird, "Composite right/left-handed leaky-wave antennas for wide-angle beam scanning with flexibly chosen frequency range," *IEEE Trans. Antennas Propag.*, vol. 68, no. 1, pp. 100–110, Jan. 2020.
[90] A. Sarkar, A. Sharma, A. Biswas, and M. J. Akhtar, "Compact CRLH leaky-wave antenna using TE20-mode substrate-integrated waveguide for broad space radiation coverage," *IEEE Trans. Antennas Propag.*, vol. 68, no. 10, pp. 7202–7207, Oct. 2020.
[91] S. Lim, C. Caloz, and T. Itoh, "Metamaterial-based electronically controlled transmission-line structure as a novel leaky-wave antenna with tunable radiation angle and beamwidth," *IEEE Trans. Microw. Theory Techn.*, vol. 53, no. 1, pp. 161–172, Dec. 2005.
[92] S. Lim, C. Caloz, and T. Itoh, "Electronically scanned composite right/left handed microstrip leaky-wave antenna," *IEEE Microw. Wireless Compon. Lett.*, vol. 14, no. 6, pp. 277–279, Jun. 2004.
[93] A. Suntives and S. V. Hum, "A fixed-frequency beam-steerable half-mode substrate integrated waveguide leaky-wave antenna," *IEEE Trans. Antennas Propag.*, vol. 60, no. 5, pp. 2540–2544, May 2012.
[94] A. Suntives and S. V. Hum, "An electronically tunable half-mode substrate integrated waveguide leaky-wave antenna," in *Proc. 5th Eur. Conf. Antennas Propag.*, 2011, pp. 3670–3674.
[95] N. Javanbakht, R. E. Amaya, J. Shaker, and B. Syrett, "Fixed frequency beam-scanning HMSIW-based leaky-wave antenna composed of circular slots in V-shape configuration," *IEEE Access*, vol. 9, pp. 52891–52901, 2021.
[96] D. K. Karmokar, K. P. Esselle, and S. G. Hay, "Fixed-frequency beam steering of microstrip leaky-wave antennas using binary switches," *IEEE Trans. Antennas Propag.*, vol. 64, no. 6, pp. 2146–2154, Jun. 2016.
[97] D. K. Karmokar, D. N. P. Thalakotuna, K. P. Esselle, L. Matekovits, and M. Heimlich, "Reconfigurable half-width microstrip leaky-wave antenna for fixed-frequency beam scanning," in *Proc. 7th Eur. Conf. Antennas Propag.*, vol. 1, 2013, pp. 1314–1317.
[98] D. K. Karmokar, D. N. P. Thalakotuna, K. P. Esselle, M. Heimlich, and L. Matekovits, "Fixed-frequency beam steering from a stub-loaded microstrip leaky-wave antenna," in *Proc. Int. Symp. Electromagn. Theory (EMTS)*, 2013, pp. 436–439.
[99] M. K. Mohsen, M. S. M. Isa, A. A. M. Isa, M. K. Abdulhameed, and M. L. Attiah, "Achieving fixed-frequency beam scanning with a microstrip leaky-wave antenna using double-gap capacitor technique," *IEEE Antennas Wireless Propag. Lett.*, vol. 18, no. 7, pp. 1502–1506, Jul. 2019.
[100] Y. Geng, J. Wang, Y. Li, Z. Li, M. Chen, and Z. Zhang, "Radiation pattern-reconfigurable leaky-wave antenna for fixed-frequency beam steering based on substrate-integrated waveguide," *IEEE Antennas Wireless Propag. Lett.*, vol. 18, no. 2, pp. 387–391, Feb. 2019.
[101] Y. Ji, L. Ge, J. Wang, Q. Chen, and W. Wu, "Simple beam scanning SIW cavity-backed slot antenna using postloaded varactor," *IEEE Antennas Wireless Propag. Lett.*, vol. 18, no. 12, pp. 2761–2765, Dec. 2019.
[102] Z. Li, Y. J. Guo, S.-L. Chen, and J. Wang, "A period-reconfigurable leaky-wave antenna with fixed-frequency and wide-angle beam scanning," *IEEE Trans. Antennas Propag.*, vol. 67, no. 6, pp. 3720–3732, Jun. 2019.
[103] X. Li, J. Wang, Z. Li, Y. Li, M. Chen, and Z. Zhang, "Dual-beam leaky-wave antenna array with capability of fixed-frequency beam switching," *IEEE Access*, vol. 8, pp. 28155–28163, 2020.
[104] I. Serhsouh, M. Himdi, H. Lebbar, and H. Vettikalladi, "Reconfigurable SIW antenna for fixed frequency beam scanning and 5G applications," *IEEE Access*, vol. 8, pp. 60084–60089, 2020.
[105] T. Lou, X.-X. Yang, H. Qiu, Q. Luo, and S. Gao, "Low-cost electrical beam-scanning leaky-wave antenna based on bent corrugated substrate integrated waveguide," *IEEE Antennas Wireless Propag. Lett.*, vol. 18, no. 2, pp. 353–357, Feb. 2019.
[106] K. Chen, Y. H. Zhang, S. Y. He, H. T. Chen, and G. Q. Zhu, "An electronically controlled leaky-wave antenna based on corrugated SIW structure with fixed-frequency beam scanning," *IEEE Antennas Wireless Propag. Lett.*, vol. 18, no. 3, pp. 551–555, Mar. 2019.
[107] H.-H. Lv, Q.-L. Huang, J.-Q. Hou, and X.-W. Shi, "Fixed-frequency beam-steering leaky-wave antenna with switchable beam number," *IEEE Antennas Wireless Propag. Lett.*, vol. 19, no. 12, pp. 2077–2081, Dec. 2020.
[108] R. Shaw and M. K. Mandal, "Broadside scanning fixed frequency LWA with simultaneous electronic control of beam angle and beamwidth," *IEEE Trans. Antennas Propag.*, vol. 68, no. 5, pp. 3504–3514, May 2020.
[109] B. Xi, Y. Li, Z. Liang, S. Zheng, Z. Chen, and Y. Long, "Periodic fixed-frequency staggered line leaky wave antenna with wide-range beam scanning capacity," *IEEE Access*, vol. 7, pp. 146693–146701, 2019.
[110] S.-L. Chen, D. K. Karmokar, P.-Y. Qin, R. W. Ziolkowski, and Y. J. Guo, "Polarization-reconfigurable leaky-wave antenna with continuous beam scanning through broadside," *IEEE Trans. Antennas Propag.*, vol. 68, no. 1, pp. 121–133, Jan. 2020.
[111] A. Iftikhar, M. Ur-Rehman, M. F. Shafique, U. Farooq, M. S. Khan, S. M. Asif, A. Fida, B. Ijaz, M. N. Rafique, and M. J. Mughal, "Planar SIW leaky wave antenna with electronically reconfigurable E- and H-plane scanning," *IEEE Access*, vol. 7, pp. 171206–171213, 2019.

NIMA JAVANBAKHT (Member, IEEE) received the B.Sc. and M.Sc. degrees in electrical engineering from the Ferdowsi University of Mashhad, Mashhad, Iran, in 2013 and 2016, respectively, and the Ph.D. degree in electrical engineering from Carleton University, Ottawa, ON, Canada, in 2021.

From 2020 to 2021, he was a Research Intern at the National Research Council Canada (NRC). Since 2021, he has been a Postdoctoral Research Fellow with the Department of Electronics, Carleton University. He has authored more than 20 technical articles in journals and more than 20 technical papers in conference proceedings. His research interests include the analysis and design of leaky-wave antennas, sidelobe suppression, reconfigurable antennas, phased array antennas, scalable antennas, compact microwave sensors, and 5G mm-wave communication devices.

Dr. Javanbakht's awards and honors include the Ontario Graduate Scholarship (OGS), the Doctoral Excellence Award, the Epstein Foundation Scholarship, and the CUASA Scholarship.

BARRY SYRETT (Member, IEEE) received the B.Eng. and M.Eng. degrees in electrical engineering from Carleton University, Ottawa, ON, Canada, in 1971 and 1973, respectively, and the Ph.D. degree in electrical engineering from the University of Alberta, Edmonton, AB, Canada, in 1976.

In 1976, he joined the Applied Instrumentation Laboratory, Department of Electronics, Carleton University, as a Senior Research Engineer, where he was involved in developing prototype electronic instrumentation systems. Since 1977, he has been with the Department of Electronics, Carleton University, where he is currently a Professor of electrical engineering. He was a Senior Industrial Fellow with Bell-Northern Research, Ottawa, in 1983 and 1991. He was involved in the development of microwave radio systems. He was a Guest Scientist with the Institute for Information Technology, National Research Council, Ottawa, in 1991. He was involved in optical interconnects. He was with the Institute for Microstructural Sciences, National Research Council, Ottawa, in 2001, where he was involved in photonic switches. He holds two patents in the area of microwave circuits. His current research interests include optoelectronic devices, monolithic microwave integrated circuits, photonic control of microwave circuits, and RF/microwave applications of metamaterials. He is a Registered Professional Engineer in the province of ON, Canada.

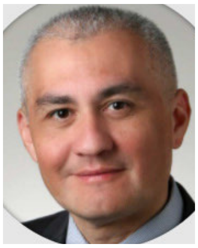

RONY E. AMAYA (Senior Member, IEEE) received the M.Eng. and Ph.D. degrees in electrical engineering from Carleton University, Ottawa, ON, Canada, in 2001 and 2005, respectively.

He joined the Design Center, Skyworks Solutions, Ottawa, in 2003, as a Senior Engineer, where he was involved in the design of RFIC for wireless transceivers. From 2006 to 2015, he was a Research Scientist with the Communications Research Centre Canada, where he was involved in developing integrated RF circuit and system solutions from S-band to E-band and addressing packaging integration. He is currently an Associate Professor with the Department of Electronics, Carleton University. He has authored or coauthored more than 60 technical articles in journals, more than 60 technical papers in conference proceedings, and holds several patents. His research interests include intelligent wireless communications systems making use of enabling microwave/RF technologies, such as smart engineered surfaces, gallium nitride and metamaterials, wireless power transfer, contactless communication links, power harvesting with applications to RFID and the IoT systems, monolithic integrated Si/GaN/GaAs circuits, high-performance microwave circuit packaging, integrated active antennas, low temperature co-fired ceramics, and micro-electro-mechanical systems.

Dr. Amaya is a member of the Association of Professional Engineers of Ontario.

JAFAR SHAKER (Senior Member, IEEE) received the B.Sc. degree in electrical engineering from the Iran University of Science and Technology, Tehran, Iran, in 1987, and the Ph.D. degree from the University of Manitoba, Winnipeg, MB, Canada, in 1995.

He has been a Research Scientist with the Communications Research Center, Ottawa, ON, Canada, since 1996. He is currently an Adjunct Professor with Carleton University, Ottawa, and the Royal Military College of Canada, Kingston, ON. He has authored or coauthored more than 50 technical articles in journals and more than 50 technical papers in conference proceedings. His current research interests include periodic structures, reflect-array, frequency selective surfaces (FSS), quasi-optical techniques, electronic band-gap structures, leaky-wave antennas, and the application of optical concepts in microwave and antenna engineering.

Dr. Shaker is a member of the Association of Professional Engineers of Ontario.